ELSEVIER

Tritium release behavior from the graphite tiles used at the dome unit of the W-shaped divertor region in JT-60U

K. Katayama [a,*], T. Takeishi [a], Y. Manabe [a], H. Nagase [a], M. Nishikawa [a], N. Miya [b]

[a] Department of Advanced Energy Engineering Science, Interdisciplinary Graduate School of Engineering Sciences, Kyushu University, Hakozaki 6-10-1, Higashi-ku, Fukuoka 812-8581, Japan
[b] Naka Fusion Research Establishment, Japan Atomic Energy Research Institute, 801-1, Naka-machi, Naka-gun, Ibaraki-ken 311-01, Japan

Abstract

Release behavior of tritium from the graphite tiles used at dome top and inner dome wing in JT-60U was investigated by the thermal desorption method in dry argon, argon with oxygen and water vapor, or argon with hydrogen. It was found that approximately 20–40% of total tritium is left in graphite even after heating to the high temperature above 1000 °C in dry argon. The residual tritium could be removed by exposing the graphite tile to oxygen with water vapor or hydrogen at the high temperature above 1000 °C. The tritium retention of the dome top tile was quantified as 84–30 kBq/cm^2. The inner dome wing tile had a steep tritium distribution from 8 to 0.1 kBq/cm^2. It is observed that a measurable amount of tritium existed in the deep site of the graphite tile.
© 2004 Elsevier B.V. All rights reserved.

PACS: 52.40.Hf

1. Introduction

In a D–T fusion reactor where graphite materials are used as plasma facing materials, tritium will be trapped to graphite materials or graphite co-deposition layers by various reactions as thermal absorption, implantation and formation of the co-deposition layers with carbon and tritium [1–3]. It is important to understand the release behavior of tritium trapped to graphite from view-points of fuel recycling and radiation safety. Many studies on tritium removal from graphite tile have been performed so far and various techniques such as laser heating method [4–6], glow discharge method with hydrogen isotope or oxygen [7–9], and oxidation method with pure oxygen gas, air or water vapor [10–17], have been proposed and tried for the graphite tiles used during D–T or D–D operation of tokamak machines such as JET, TFTR or TEXTOR. Most previous experiments have focused on removal of tritium from the co-deposition layer or removal of the co-deposition layer itself at the temperature range from 200 °C to 500 °C targeting on in situ cleaning. During plasma discharge, tritium has extensive energy distribution and it is implanted into the depth of graphite grain corresponding to its energy

* Corresponding author. Tel.: +81 92 642 3785; fax: +81 92 642 3784.
E-mail address: kadzu@nucl.kyushu-u.ac.jp (K. Katayama).

[18–23]. Therefore, the high-energy (~ 1 MeV) tritium generated by D–D nuclear reaction is deeply implanted into plasma facing side of graphite grain. In order to evaluate tritium retention in whole graphite tile strictly and to detritiate the used graphite tile effectively down to the practicable level to reuse or to dispose as the low level radioactive waste, it is necessary to remove tritium from not only the co-deposition layer but also the substrate graphite grain.

D–D experiments have been performed in JT–60U at Japan Atomic Energy Research Institute (JAERI), and the tritium produced by the D–D nuclear reaction was retained in plasma facing graphite tiles. It has been reported the tritium retained in the divertor and the first wall were 10% and 40% of the generated tritium, respectively [24]. Additionally it has been revealed by simulation using the orbit following Monte Carlo (OFMC) code that about 30% of energetic triton is implanted to the graphite tiles [25,26]. A detailed surface profile of tritium in the divertor region has been investigated recently by the tritium imaging plate technique (TIPT) that can detect tritium distributed within a depth of about 3.5 μm from the surface of graphite tiles [25,27]. An approximate distribution of tritium in the divertor region has been also investigated by full combustion of graphite pieces that was cut from the used graphite tiles [25]. It has been indicated in these papers that the tritium level has a large difference from the dome top tile to the inner dome wing tile. In this study, tritium retained in the graphite tiles used as dome top tile and inner dome wing tile in D–D experiments of JT–60U was removed by the thermal desorption method in dry argon where the temperature is elevated to above 1000°C. After the thermal desorption operation, the graphite tiles was exposing to the mixed gas of oxygen and water vapor carried with argon, or dry hydrogen carried with argon to investigate the amount of residual tritium. From the beginning temperature of tritium release in the thermal desorption operation, the relation of tritium retention and the surface temperature of graphite tiles during plasma discharge was discussed. Additionally, appropriate depth profiles of tritium in the graphite tile were investigated.

2. Experimental

2.1. Tritium removal experiment

2.1.1. Sample tiles

The sample tiles used in this study are the dome top tile (5DM2bp) and the inner dome wing tile (5DM2ap) in the W-shaped divertor region of JT–60U. Fig. 1 shows poloidal position of analyzed graphite tiles. The dome top tile consists of carbon fiber composite (PCC-2S) and the inner dome wing tile consists of isotropic graphite (IG-430U). These tiles were exposed to about 3600
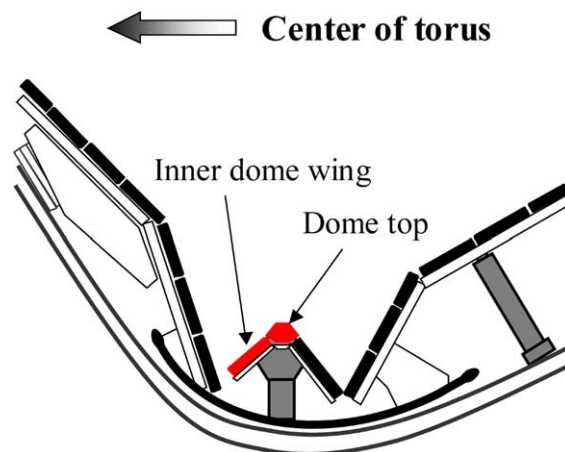

Fig. 1. Poloidal position of the dome top tile and the inner dome wing tile in the W-shaped divertor region.

deuterium plasma discharges for the operation periods, June 1997–October 1998. After the deuterium plasma operation, about 700 hydrogen plasma discharges were performed to decontaminate the surface tritium. Accordingly it is considered that the surface tritium had been already disappeared by hydrogen plasma discharges and following air ventilation before we received the graphite tiles. The re-deposition layer of nearly 20 μm thickness has been observed on the inner dome wing at least in the zone close to the dome top and no continuous re-deposition layer has been observed on the dome top [28]. However, it has been already reported that there is no correlation between the re-deposition layer and the tritium retention in JT–60U [3,25].

The graphite tiles were cut into some pieces and those pieces was named as shown in Fig. 2. For measurement of the depth profile of tritium in graphite tile, 3B was cut into 3 pieces at about 2 mm intervals to the depth direction and these pieces were named 3B1, 3B2 and 3B3. Also 9B was cut into 3 pieces at about 5 mm, 5 mm and 10 mm to the depth direction and these pieces were named 9B1, 9B2 and 9B3. For measurement of tritium trapped in the shallower part of tile, 9A was sanded to the depth of about 150 μm from plasma facing side and all powders were used as sample 9A1. The remnant of piece 9A was cut at about 7 mm from plasma facing side and named 9A2. All pieces except 9A1 were crushed into granules and then particles of 0.35–1.4 mm were used as experimental samples.

2.1.2. Experimental apparatus

The schematic diagram of the apparatus used for tritium removal experiments is shown in Fig. 3. The piping system consists of copper pipes. The reaction tube is made by quartz with brass joint. A cold trap, which was filled with molecular sieve 5A and cooled with ice
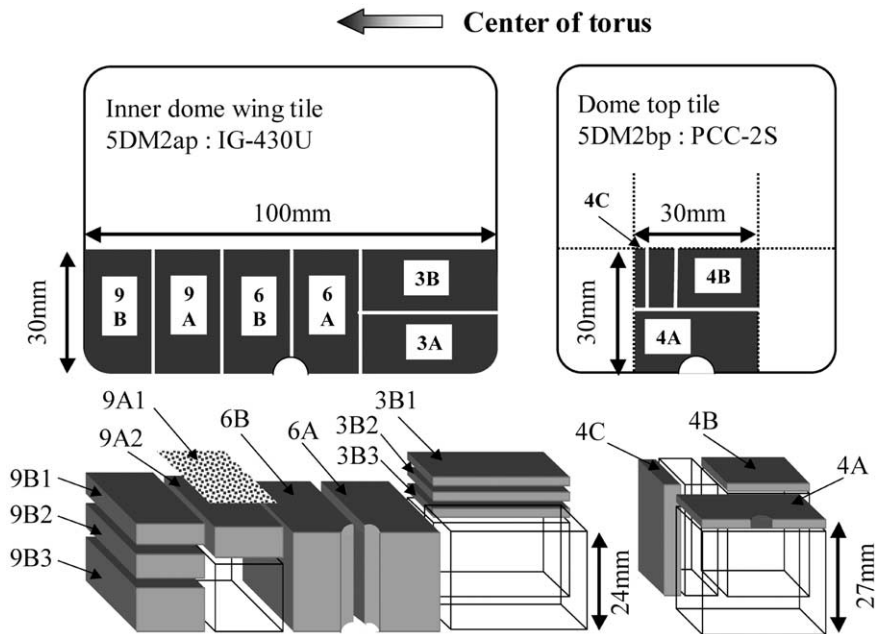
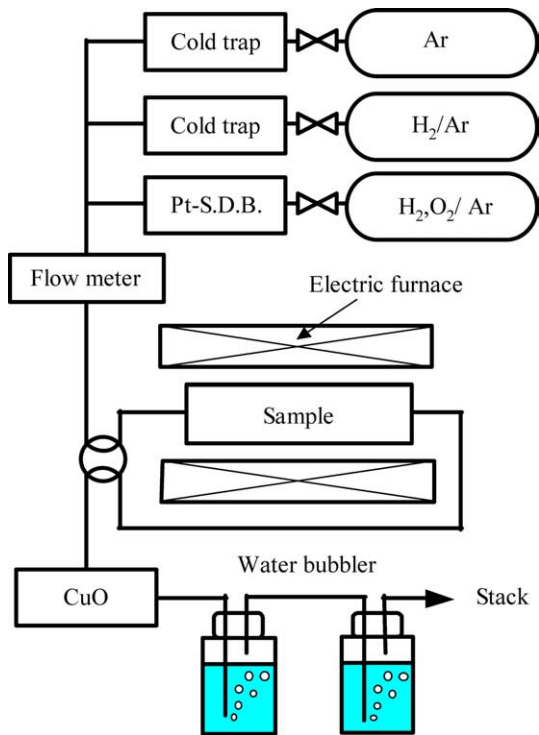Fig. 2. Locations and sizes of samples cut in toroidal direction and schematic diagram of sample shape.

Fig. 3. Schematic diagram of the experimental apparatus.

water, was used to remove water vapor from the process gas. A pure argon gas, an argon gas containing hydro-

gen of 500 Pa, and an argon gas containing oxygen of 5000 Pa and hydrogen of 1000 Pa were used in this experiment. Hereafter a pure argon gas passed through a cold trap, and an argon gas containing hydrogen of 500 Pa passed through a cold trap are called as a dry argon gas and a dry hydrogen gas, respectively. With the Pt-SDB (Styrene Divinyl Benzene) catalyst bed at the room temperature, an argon gas containing oxygen and hydrogen was converted to an argon gas containing oxygen of 4500 Pa and water vapor of 1000 Pa which is called as a wet oxygen gas hereafter. A CuO bed was heated to 300 °C to convert gaseous tritium to tritiated water. The tritiated water was collected in water bubblers and tritium concentration was measured using a liquid scintillation counter. This apparatus is equipped with two bubblers to collect the released tritium. However, for all experiments the tritium concentration of the second bubbler did not increase. This indicates that all the released tritium was trapped in the first bubbler. The gas flow rate was kept 180 ml/min by a mass flow meter. The sample bed was heated to the experimental temperature by an electric furnace.

2.1.3. Experimental operation

Specifications of samples and experimental conditions are shown in Table 1. The experiments were carried out as follows. Sample 4A, 3B1, 6B, 9A1 and 9B1 were heated from room temperature to 200 °C and then stepwise heated from 200 °C to 1200 °C in 100 °C steps at 1-h intervals. During the heating operation a dry argon gas was passed through the sample bed. In

Table 1
Specifications of samples and experimental conditions

Sample name	Weight (g)	Thickness (mm)	Plasma facing area (mm²)	Temperature (°C)	Heating rate	Material
4A	1.347	2	418	1200	Stepwise	CFC
4B	1.300	2	300	1000	Quickly	CFC
4C	1.485	27	50	1000	Quickly	CFC
3B1	1.385	2	495	1200	Stepwise	IG
3B2	1.658	2	495	1000	Quickly	IG
3B3	2.157	2	495	1000	Quickly	IG
6A	15.18	24	479	1200	Quickly	IG
6B	15.85	24	479	1200	Stepwise	IG
9A1	0.485	0.15	495	1200	Stepwise	IG
9A2	4.963	6.7	495	1000	Quickly	IG
9B1	3.895	5	495	1200	Stepwise	IG
9B2	4.769	5.7	495	1000	Quickly	IG
9B3	7.914	11	495	1000	Quickly	IG

parallel, tritiated water of 1.0 ml was sampled from the bubbler at hourly intervals. Sample 6A was quickly heated to 1000 °C where the sample bed was closed at a dry argon atmosphere. After the temperature was attained at 1000 °C, a dry argon gas was introduced to sample bed and the tritiated water in the bubbler was periodically sampled. Sample 4B, 4C, 3B2, 3B3, 9B2, 9B3 and 9A2 were quickly heated to 1000 °C. During the heating operation a dry argon gas was passed through the sample bed. The tritiated water in the bubbler was periodically sampled.

For sample 3B1 and 6A, a wet oxygen gas was introduced to the sample bed after the heating operation mentioned above. For other samples, a dry hydrogen gas was introduced to the sample bed at first and introduction of a wet oxygen gas was followed.

2.1.4. Water-soak test

Graphite powder generated from 4A piece was soaked in water to investigate tritium release at room temperature. Tritium concentration of the water was measured using a liquid scintillation counter after 7 months.

2.2. Erosion measurement

The weight loss of graphite when exposed to a wet oxygen gas or a dry hydrogen gas was measured to estimate the erosion rate of graphite in the tritium removal experiments mentioned above. Isotropic graphite (IG-430U by Toyo Tanso Co.), which was not used in the experiment of JT-60, was crushed into granules and then particles of 1.0–1.4 mm were packed in a quartz reaction tube. Graphite particles were heated to 1000 °C or 1200 °C in a dry argon atmosphere and then a wet oxygen gas or a dry hydrogen gas was introduced to the sample bed with 180 ml/min which is equal to the gas flow rate in the tritium removal experiments. Weight changes of graphite were measured with an electric bal-

ance with a sensitivity of 0.01 mg, against a weight of graphite sample of about 1 g.

3. Results and discussion

No tritium was detected in the water in which the graphite powder was soaked for 7 months. This fact certifies that tritium is no longer released at room temperature. It is considered that the tritium existing in the shallow region of the graphite grain has been already released during storage for a few years in addition to hydrogen plasma discharges and air ventilation.

A release behavior of tritium from sample 3B1 is shown in Fig. 4. The release rate of tritium increases gradually with increasing temperature. When a wet oxygen gas is introduced to the sample bed after decreasing the release rate, a large amount of tritium is released within one hour. The amount of tritium reaches approximately 40% of total tritium released from this sample. It is remarkable that such a large amount of tritium is still left in graphite after the thermal desorption operation in
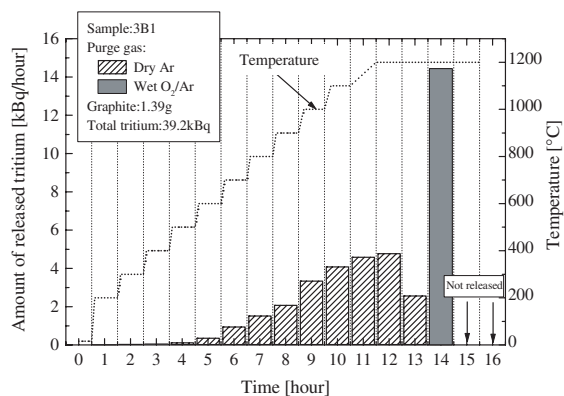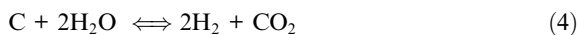

Fig. 4. Amount of tritium released from sample 3B1 per hour.

dry argon at a high temperature of 1200 °C. A similar release curve of tritium has been observed by Shu et al. [17] in the tritium release experiment from the co-deposition layers formed on graphite tiles used in D–T experiment of TFTR. In the layer, the tritium release rate increased rapidly when purging gas was shifted from a pure argon gas to an argon gas containing 1% oxygen, after the tritium release rate by the thermal desorption at 240 °C decreased. The authors have mentioned that the chemical erosion with oxidation of the co-deposition layer enhanced the tritium release. It is considered that the increase of tritium release rate observed in our work is also mainly due to the erosion of graphite with oxygen and water vapor. Studies on the reaction between carbon and oxygen have been carried out and the erosion rate of graphite at wide temperature region is summarized as the erosion yield, C/O_2 [29]. Carbon and water vapor reactions at high temperature have been also studied from several viewpoints such as a safety of fusion rector with regard to loss of coolant inside the vacuum vessel [30–32], erosion of carbon based material used as gas turbine blades or scramjet combustors [33,34] and gasification of coal, coke or carbon with water vapor [35]. It is considered from those earlier studies that graphite would be eroded by following reactions with oxygen,

$$C + 1/2\,O_2 \iff CO \tag{1}$$

$$C + O_2 \iff CO_2 \tag{2}$$

and following reactions with water vapor,

$$C + H_2O \iff CO + H_2 \tag{3}$$

$$C + 2H_2O \iff 2H_2 + CO_2 \tag{4}$$

Carbon dioxide generated by carbon–oxygen or carbon–water vapor reaction would also act as a reactant in the following reaction,

$$C + CO_2 \iff 2CO \tag{5}$$

Additionally, a part of tritium appeared on the surface of graphite grain by thermal diffusion and by erosion of graphite might be immediately released as tritiated water via the following isotope exchange reaction [36,37],

$$T\ (\text{surface}) + H_2O\ (\text{gas phase})$$
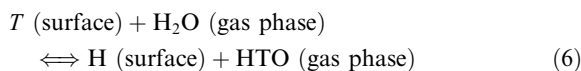$$\iff H\ (\text{surface}) + HTO\ (\text{gas phase}) \tag{6}$$

Fig. 5 shows weight changes of graphite when exposed to a wet oxygen gas and a dry hydrogen gas at temperatures of 1000 °C and 1200 °C. It was confirmed that graphite is eroded by the purging operation with a wet oxygen gas. On the other hand, weight changes by the purging operation with a dry hydrogen gas were not observed. The erosion rates of graphite by exposing
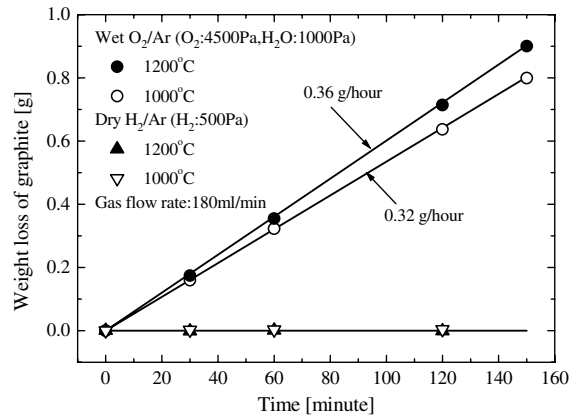

Fig. 5. Weight loss of isotropic graphite (IG-430U).

to a wet oxygen gas at temperatures of 1000 °C and 1200 °C can be obtained to be constant as 0.32 g/h and 0.36 g/h, respectively. If the erosion rate is dominated by the diffusion in the pores of graphite, it becomes large with time, because the pore size becomes large as the erosion proceeds. Since the obtained erosion rate is constant, a reaction on the grain surface is considered to be a rate-determination step in the mass transfer for the erosion reaction. The following relation holds when a sphere grain is assumed,

$$(d/d_0)^3 = M/M_0, \tag{7}$$

where d is the diameter of eroded grain [μm], d_0 is the initial diameter of grain [μm], M is the weight of eroded graphite [g] and M_0 is the initial weight of graphite [g]. An equivalent grain diameter of IG-430U is determined to be about 9 μm from SEM observation. When the initial diameters of all grains composing graphite granules of sample 3B1 are assumed to be 9 μm, the diameters of grains eroded during the purging operation with a wet oxygen gas for 1 h are calculated from Eq. (7) to be approximately 8.14 μm. That is to say, the released tritium seems to be left within the depth of 0.86 μm from the surface of graphite grain.

A typical release behavior of tritium when sample graphite was stepwise heated to 1200 °C in a dry argon gas and then a dry hydrogen gas was introduced to sample bed is shown in Fig. 6 where the result for sample 4A is represented. A large amount of tritium was immediately released similarly to the case that a wet oxygen gas was introduced. The release rate of tritium by introducing a dry hydrogen gas was slightly slower than that by introducing a wet oxygen gas. Similar histograms were observed for sample 6B, 9A, and 9B1, which were performed same experimental operation, although total tritium released from each sample was different. If tritium was being trapped on the surface of piping system, which is always at room temperature, the tritium cannot
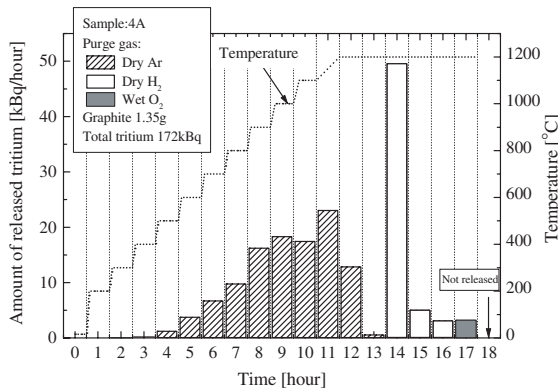
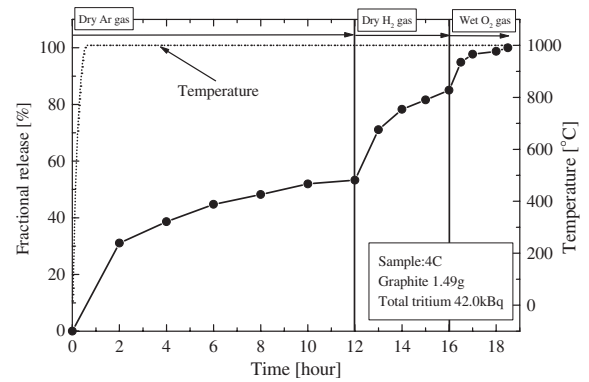Fig. 6. Amount of tritium released from sample 4A per hour.

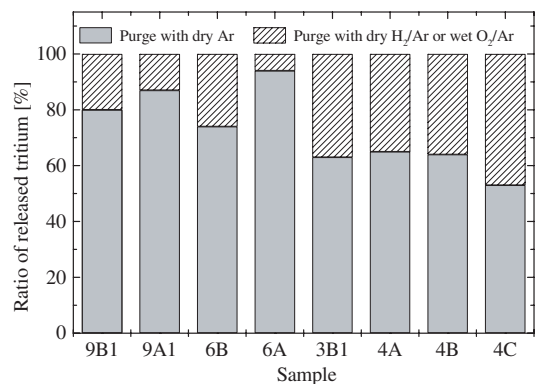Fig. 7. Sequential release curve of tritium from sample 4C.

Fig. 8. Ratios of the amount of tritium released by the purging operation with a dry argon gas, and a dry hydrogen gas or a wet oxygen gas at a temperature of 1000 °C or 1200 °C.

be released by the purging operation with a dry hydrogen gas because the overall mass transfer coefficient of the isotope exchange reaction between tritium on the surface of copper and gaseous hydrogen in a gas phase is very small at room temperature [37]. Therefore, it is considered that tritium was released from not piping system but the sample bed. Graphite erosion with a dry hydrogen gas does not occur in high temperatures of 1000 °C and 1200 °C indicated in Fig. 5. That is to say, the tritium released by the purging operation with a dry hydrogen gas is not due to graphite erosion. We consider that tritium was released by an effect of the isotope exchange reaction with hydrogen. However, the state of tritium left in graphite after the thermal desorption operation in dry argon at 1200 °C is not clear. The further research for tritium release from graphite is required. In all cases, two types of tritium were observed. One can be removed by heating in dry argon and the other cannot easily removed only by heating in dry argon. Latter tritium gives remarkable effect on tritium inventory and is necessary to be considered for establishing tritium decontamination technique.

An example of sequential release curve of tritium from graphite is shown in Fig. 7, where the result for sample 4C is represented. Sample graphite was continuously exposed to a dry argon gas, a dry hydrogen gas and a wet oxygen gas at a temperature of 1000 °C. The fractional release in this figure is normalized with the total amount of tritium released from this sample. As this figure indicates, the tritium removal only by heating in dry argon seems very difficult, because the release rate of tritium becomes much slower at 12 h after the operation is started, although approximately 50% of tritium is left in graphite. In order to remove tritium effectively without erosion of graphite, it is necessary to expose graphite to hydrogen at a high temperature as 1000 °C.

Fig. 8 compares ratios of the amount of tritium released by the purging operation with a dry argon gas,

and a dry hydrogen gas or a wet oxygen gas at a temperature of 1000 °C or 1200 °C. It was found that approximately 20% of total tritium was left in graphite for sample 6B, 9A1 and 9B1. Also approximately 40% of total tritium was left in graphite for sample 3B1, 4A, 4B and 4C. For sample 6A, however, no more than 6% was released by the purging operation with a wet oxygen gas. The ratio of the residual tritium after the purging operation with a dry argon gas does not likely to depend on difference in tritium retention and difference in material, although the inner dome wing tile is isotropic graphite and the dome top tile is CFC graphite. The difference of the ratio may relate to the emission of other hydrogen isotopes. That is to say, the isotope exchange reaction between the tritium remaining in graphite and the hydrogen released to the gas phase may have occurred in the reaction tube. Presumably, in the case of 6A the isotope exchange reaction proceeded sufficiently in the closed reaction tube because the released hydrogen isotopes accumulate at high temperature of

1000 °C till the reaction tube is opened at about 1-h intervals. It is likely that we need to investigate the retention and release behavior of hydrogen and deuterium together with tritium in order to discuss the ratio of the residual tritium after the thermal desorption operation in dry argon.

The beginning parts of tritium release curves by the thermal desorption operation in dry argon for sample 4A, 3B1, 6B, 9A1 and 9B1 are shown in Fig. 9. We decided to consider the experimental error that tritium release started when total amount of tritium reached 50 Bq shown in this figure by a chain line. The temperature, which is expressed by a thick line, is smoothed for estimation of the onset of release. The lines connecting each experimental point are guide to the eyes. It was found that the beginning temperature of tritium release rises from the dome top to the edge of the inner dome wing tile as shown in Fig. 6. Sample 4A, which is located in dome top, released tritium at the lowest temperature of 75 °C among the samples. At the edge of inner dome wing tile opposite to the dome top side, tritium was released at the maximum temperature of 480 °C. It is considered that these beginning temperatures reflect the surface temperatures of each region on the tile during plasma discharge in the final period because the tritium that can be released below at tile temperature during plasma discharge has already released to the gas phase in the vacuum vessel of JT-60U. The temperature of the inner dome wing tile during plasma discharge has been measured by the thermocouple installed at 6 mm depth and reported that its temperature changes from 300 to 400 °C where the temperature of 300 °C is a base temperature of plasma facing tiles [25]. Our estimated temperatures for 6B and 9A1, which is located in about center of the inner dome wing tile, are relatively close to the thermocouple data. It is indicated from our estimations that the inner dome wing tile has a sharp temperature distribution from 200 °C to 480 °C and the
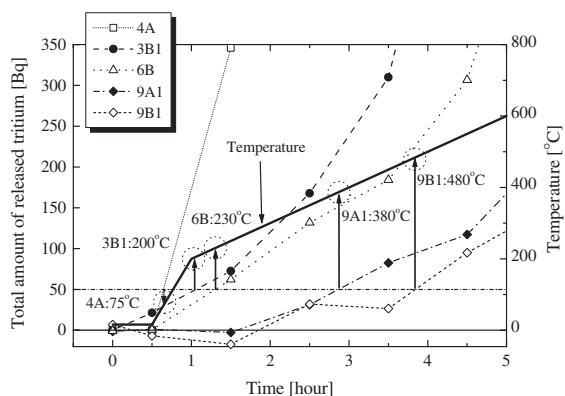
temperature of the dome tope tile is below 100 °C during plasma discharge.

The amount of tritium released from the samples containing plasma facing surface are compared in Fig. 10 where the ordinate indicates tritium amount per plasma facing area of each sample [kBq/cm^2] and the square plot shows the release beginning temperature obtained from Fig. 9. It is observed that the tritium retention falls off between the dome top tile and the inner dome wing tile and then sharply decreases toward the edge of the inner dome wing tile. The tritium retentions of the dome top tile were obtained as 84–30 kBq/cm^2. Masaki et al. has measured the tritium retention of the dome top tile, which was located next to the tile analyzed by the present authors and was used in the same discharge period, by full combustion method [25]. The tritium retention of the tile has been reported to be 60 kBq/cm^2. The tritium retentions obtained by the present authors agree with the value measured by Masaki et al. This agreement indicates that our experimental process could remove the whole tritium retained in the tile successfully. It is found that the inner dome wing tile has a steep tritium distribution. The amount of tritium in the part close to the dome top is about 8 kBq/cm^2, on the contrary the amount of tritium in the opposite side is much lower and its value is about 0.1 kBq/cm^2. As can be seen from this figure, the tritium distribution shows a reverse tendency to the beginning temperature of tritium release. In other words, the amount of tritium retained in those tiles seems to depend strongly on the tile temperature during plasma discharge. It has been experimentally obtained that the saturated hydrogen retention of graphite by ion irradiation decreases with increasing temperature during irradiation [20,21,38]. Also Tanabe et al. have pointed out for the tritium distribution of JT-60U tiles that the tritium once implanted is redistributed by the temperature increase due to the plasma heat load [27]. However, tritium retention depends not only on temperature but also on the particle flux of energetic triton.

Fig. 9. Beginning parts of tritium release curves by the thermal desorption operation in dry argon for sample 4A, 3B1, 6B, 9A1 and 9B1.
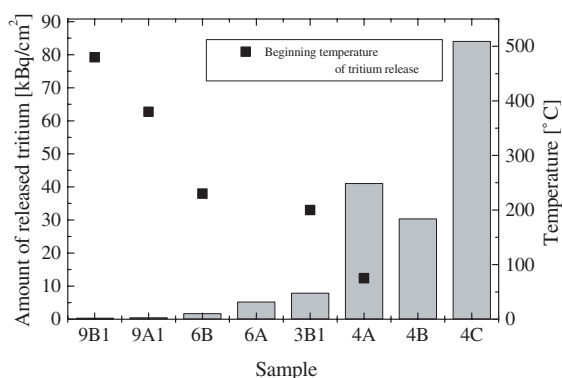

Fig. 10. Tritium distribution from the dome top to the inner dome wing with the beginning temperature of tritium release.
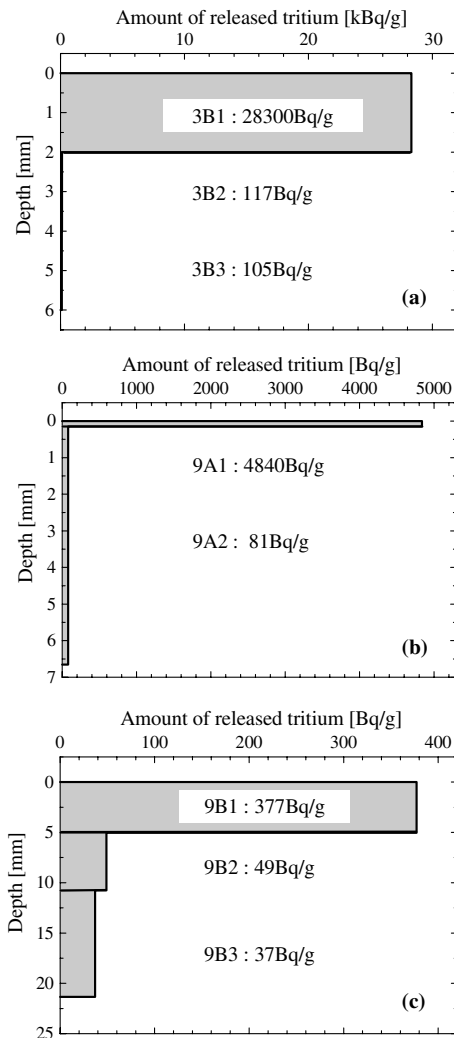
Fig. 11. Depth profiles of tritium in graphite tile for block 3B (a), 9A (b) and 9B (c).

Table 2
Summary of total tritium released from each sample and release beginning temperature

Sample name	Released tritium (Bq)	Release beginning (°C)
4A	172 000	75
4B	91 200	–
4C	42 000	–
3B1	39 200	200
3B2	194	–
3B3	227	–
6A	25 200	–
6B	8270	230
9A1	2350	380
9A2	402	–
9B1	1470	480
9B2	235	–
9B3	294	–

Masaki et al. have calculated the particle flux of energetic triton to the divertor region using the OFMC code and it has been reported that the particle flux at the dome top is largest in the divertor region and that at the inner dome wing is much lower than that at the dome top [25]. From those results tritium distribution would be formed as follows. At the dome top, a relatively large amount of tritium is implanted to the plasma facing surface of graphite grain and most of them would remain there because the implanted tritium can hardly diffuse in the grain since temperature is low. On the other hand at the inner dome wing, a relatively small amount of tritium is implanted to the plasma facing surface of graphite grain and then a part of them would be released to the gas phase because the implanted tritium can diffuse in the grain since temperature is high. The tendency of tritium distribution from the inner dome wing to the dome top is in agreement with that obtained using TIPT by Tanabe et al. [27], although TIPT cannot detect the tritium retained beyond a depth of 3.5 μm. This agreement indicates that a large amount of tritium is retained within a depth of 3.5 μm.

Approximate depth profiles of tritium in the graphite tile were investigated for block 3B, 9A and 9B. These results are shown in Fig. 11(a)–(c) where the amount of the released tritium is divided by the sample weight. It is observed that the tritium retention of the first pieces or the powder, which contain plasma facing surface, is much larger than that of the second and third pieces. The result for 9A indicates that a large amount of tritium exists within the depth of 150 μm. However, tritium of 37–117 Bq/g was released from the second and third pieces depending upon tritium retention in plasma facing side. This result indicates that a small amount of tritium exists measurably in the deep site of graphite tile. It is considered that tritium in molecular form deeply diffuses into graphite tile through the pores of graphite tile and then thermally penetrates into the grain. The concentration of the tritium absorbed into the bulk of the tiles is very small as shown in Fig. 11, compared with that implanted to the surface layer. Since an absorption reaction proceeds in the whole tiles, however, total amount of absorbed tritium in the vessel becomes large. We predict that the absorption of tritium into the bulk of the tiles will be one of the serious problems in future long-term D–T operation because the tritium absorbed in the deep site of the tiles cannot be removed by a discharge cleaning. The total tritium released from each sample and the estimated surface temperatures during plasma discharge are summarized in Table 2.

4. Conclusions

Release behavior of tritium from the graphite tiles used at dome top and inner dome wing in JT-60U was

experimentally investigated by the thermal desorption method in dry argon, argon with oxygen and water vapor, or argon with hydrogen. It was found that approximately 20–40% of total tritium is left in graphite even after heating to the high temperature above 1000 °C in dry argon. The residual tritium could be removed by exposing the graphite tile to oxygen with water vapor or hydrogen at high temperatures of 1000 °C and 1200 °C. It seems that two types of tritium exist in the used graphite tiles. One can be removed by heating in argon and another cannot be easily removed only by heating in argon. In order to remove tritium effectively without erosion of graphite, it is necessary to expose graphite to hydrogen at a high temperature as 1000 °C. However, it is not cleared how tritium can be left in graphite after heating at a high temperature above 1000 °C in argon and how the residual tritium can be removed by exposing graphite to hydrogen. The further research for the release behavior of tritium from graphite is required.

Tritium retention falls off sharply between the dome top tile and the inner dome wing tile. The tritium retention of the dome top tile was obtained as 84–30 kBq/cm^2. The inner dome wing tile had a steep tritium distribution from 8 to 0.1 kBq/cm^2. The tritium distribution from dome top to inner dome wing shows a inverse relation to the beginning temperature of tritium release obtained from the release curve of tritium in the thermal desorption operation in dry argon.

Tritium of 37–117 Bq/g was released from the graphite pieces which do not include plasma facing surface. The amount of tritium depended upon tritium retention in the plasma facing side. This result indicates that some amount of tritium exists measurably in deep site of graphite tile.

Acknowledgments

References

[1] P. Franzen, R. Behrisch, C. García-Rosales, ASDEX Upgrade team, D. Schleussner, D. Rösler, J. Becker, W. Knapp, C. Edelmann, Nucl. Fus. 37 (1997) 1375.

[2] R.A. Causey, J.N. Brooks, G. Federici, Fus. Eng. Des. 61&62 (2002) 525.

[3] T. Tanabe, N. Bekris, P. Coad, C.H. Skinner, M. Glugla, N. Miya, J. Nucl. Mater. 313–316 (2003) 478.

[4] C.H. Skinner, C.A. Gentile, A. Carpe, G. Guttadora, S. Langish, K.M. Young, W.M. Shu, H. Nakamura, J. Nucl. Mater. 301 (2002) 98.

[5] T.J. Venhaus, R.D. Penzhorn, R.A. Causey, N. Bekris, J. Nucl. Mater. 302 (2002) 224.

[6] Y. Oya, W. Shu, S. O'hira, T. Hayashi, H. Nakamura, T. Sakai, T. Tadokoro, K. Kobayashi, T. Suzuki, M. Nishi, J. Nucl. Mater. 290–293 (2001) 469.

[7] S. Hiroki, Y. Hasegawa, K. Kaneko, T. Abe, Y. Murakami, J. Nucl. Mater. 224 (1995) 293.

[8] B. Landkammer, A. von Keudell, W. Jacob, J. Nucl. Mater. 264 (1999) 48.

[9] W. Jacob, B. Landkammer, C.H. Wu, J. Nucl. Mater. 266 (1999) 552.

[10] A.A. Haasz, J.W. Davis, J. Nucl. Mater. 256 (1998) 65.

[11] S. Alberici, J.P. Coad, H.-K. Hinssen, R. Moormann, P. Wienhold, C.H. Wu, J. Nucl. Mater. 258–263 (1998) 764.

[12] J.W. Davis, A.A. Haasz, J. Nucl. Mater. 266–269 (1999) 478.

[13] M. Rubel, J. von Seggern, P. Karduck, V. Philipps, A. Vevecka-Priftaj, J. Nucl. Mater. 266–269 (1999) 1185.

[14] R.-D. Penzhorn, N. Bekris, W. Hellriegel, H.-E. Noppel, W. Nägele, H. Ziegler, R. Rolli, H. Werle, A. Haigh, A. Peacock, J. Nucl. Mater. 279 (2000) 139.

[15] R. Moormann, S. Alberici, H.-K. Hinssen, C.H. Wu, Fus. Eng. Des. 49&50 (2000) 295.

[16] N. Bekris, C. Caldwell-Nichols, L. Doerr, M. Glugla, R.-D. Penzhorn, H. Ziegler, J. Nucl. Mater. 307–311 (2002) 1649.

[17] W.M. Shu, C.A. Gentile, C.H. Skinner, S. Langish, M.F. Nishi, Fus. Eng. Des. 61&62 (2002) 599.

[18] M. Rubel, H. Bergsaker, P. Wienhold, J. Nucl. Mater. 241–243 (1997) 1026.

[19] W. Möller, J. Nucl. Mater. 162–164 (1989) 138.

[20] B.M.U. Scherzer, R. Behrisch, W. Eckstein, U. Littmark, J. Roth, M.K. Sinha, J. Nucl. Mater. 63 (1976) 100.

[21] R.A. Langley, R.S. Blewer, J. Roth, J. Nucl. Mater. 76&77 (1978) 313.

[22] W.R. Wampler, C.W. Magee, J. Nucl. Mater. 103&104 (1981) 509.

[23] S.A. Cohen, G.M. Mccracken, J. Nucl. Mater. 84 (1979) 157.

[24] K. Masaki, K. Kodama, T. Ando, M. Saidoh, M. Shimizu, T. Hayashi, K. Okuno, Fus. Eng. Des. 31 (1996) 181.

[25] K. Masaki, K. Sugiyama, T. Tanabe, Y. Gotoh, K. Miyasaka, K. Tobita, Y. Miyo, A. Kaminaga, K. Kodama, T. Arai, N. Miya, J. Nucl. Mater. 313–316 (2003) 517.

[26] K. Tobita, S. Nishio, S. Konishi, M. Sato, T. Tanabe, K. Masaki, N. Miya, Fus. Eng. Des. 65 (2003) 561.

[27] T. Tanabe, K. Miyasaka, K. Masaki, K. Kodama, N. Miya, J. Nucl. Mater. 307–311 (2002) 1441.

[28] Y. Gotoh, J. Yagyu, K. Masaki, K. Kizu, A. Kaminaga, K. Kodama, T. Arai, T. Tanabe, N. Miya, J. Nucl. Mater. 313–316 (2003) 370.

[29] J.W. Davis, C.G. Hamilton, A.A. Haasz, J. Nucl. Mater. 288 (2001) 148.

[30] G.R. Smolik, B.J. Merrill, S.J. Piet, D.F. Holland, Fus. Technol. 19 (1991) 1342.

[31] R. Moormann, H.K. Hinssen, A.-K. Krssenberg, B. Stauch, C.H. Wu, J. Nucl. Mater. 212–215 (1994) 1178.

[32] T. Uda, M. Ogawa, Y. Seki, T. Kunugi, I. Aoki, T. Honda, T. Okazaki, N. Nishino, Fus. Eng. Des. 29 (1995) 238.

[33] A. Makino, T. Namikiri, K. Kimura, Combust. Flame 132 (2003) 743.

[34] M.-P. Bacos, J.-L. Cochon, J.-M. Dorvaux, O. Lavigne, Carbon 38 (2000) 93.

[35] G. Hermann, K.J. Httinger, Carbon 24 (1986) 705.

[36] M. Nishikawa, N. Nakashio, T. Takeishi, S. Matsunaga, K. Kuroki, Fus. Technol. 28 (1995) 1233.

[37] K. Katayama, M. Nishikawa, Fus. Technol. 41 (2002) 53.

[38] B.L. Doyle, W.R. Wampler, D.K. Brice, J. Nucl. Mater. 103&104 (1981) 513.